arXiv:1701.06353v1 [math.NA] 23 Jan 2017

IMPROVED APPROXIMATION OF EIGENVALUES IN ISOGEOMETRIC METHODS FOR MULTI-PATCH GEOMETRIES AND NEUMANN BOUNDARIES

THOMAS HORGER, ALESSANDRO REALI, BARBARA WOHLMUTH, AND LINUS WUNDERLICH

Abstract. We present a systematic study on isogeometric approximations of second order elliptic eigenvalue problems. In the case of either Neumann boundaries or multi-patch geometries and a mortar approach spurious eigenvalues - typically referred to as "outliers" - occur. This pollution of the discrete spectrum can be avoided by a hybrid approach. In addition to the imposed weak consistency with respect to the Neumann boundary and to the interface mortar coupling condition, we apply higher-order penalty terms for the strong coupling. The mesh dependent weights are selected such that uniform continuity is guaranteed and optimal a priori estimates are preserved. Numerical results show the good behavior of the proposed method in the context of simple 1D and 2D Laplace problems, but also of more complex multi-patch mapped geometries and linear elasticity.

Isogeometric analysis, Eigenvalues, Mortar methods, Penalty methods, Multi-patch geometries, Neumann boundaries

1. Introduction

Isogeometric analysis (IGA), introduced in 2005 by Hughes et al. in [1], is a family of methods using highly regular basis functions typical of CAD systems, like B-splines or non-uniform rational B-splines (NURBS), to construct numerical approximations of partial differential equations (PDEs). The idea of using spline functions for the approximation of PDEs can even be found in earlier works (see, e.g., [2] and references therein). However, in IGA the computational domain is also represented in terms of the same functions used for approximation, in an isoparametric fashion, with the goal of vastly simplifying the mesh generation and refinement processes with respect to standard finite element analysis (FEA), possibly bridging the gap between CAD and analysis.

(T. Horger, B. Wohlmuth, L. Wunderlich) Institute for Numerical Mathematics, Technische Universität München, Boltzmannstrasse 3, 85748 Garching b. München, Germany

(A. Reali) Department of Civil Engineering and Architecture, University of Pavia, via Ferrata 3, 27100 Pavia, Italy

(A. Reali) Institute for Advanced Study, Technische Universität München, Lichtenbergstrasse 2a, 85748 Garching b. München, Germany

E-mail addresses: (T. Horger) horger@ma.tum.de, (A. Reali) alessandro.reali@unipv.it, (B. Wohlmuth) wohlmuth@ma.tum.de, (L. Wunderlich, Corresponding author) linus.wunderlich@ma.tum.de.

TH, BW, and LW would like to gratefully acknowledge the funds provided by the Deutsche Forschungsgemeinschaft under the contract/grant numbers: WO 671/11-1, WO 671/13-2 and WO 671/15-1 (within the Priority Programme SPP 1748, "Reliable Simulation Techniques in Solid Mechanics. Development of Non-standard Discretisation Methods, Mechanical and Mathematical Analysis". AR would like to gratefully acknowledge the funds provided by Fondazione Cariplo - Regione Lombardia through the project "Verso nuovi strumenti di simulazione super veloci ed accurati basati sull'analisi isogeometrica", within the program RST - rafforzamento.

Thanks to its high-regularity, IGA has also shown to possess superior approximation properties, on a per-degree-of-freedom basis, with respect to classical FEA, and has been successfully applied in many fields of computational mechanics, including the approximation of eigenvalue problems. Eigenvalue analysis arises in many important applications in science and engineering, where the amount of eigenvalues of interest can be quite different from application to application. For example in vibro-acoustics one is typically only interested in the first part of the spectrum, while for explicit dynamics the approximation quality of the entire spectrum is relevant. Compared to FEA, it was observed that IGA possesses superior approximation of eigenvalues, see [3, 4, 5, 6]. Such studies are however limited to single-patch geometries and Dirichlet boundary conditions.

In general, when dealing with non-trivial engineering applications, the isogeometric computational domain is constituted by the assembly of multiple patches and thus efficient algorithmic techniques to couple different patches are required. To retain the flexibility of the meshes at the interfaces, mortar methods are a very attractive option, originally introduced for the coupling of non-matching meshes in spectral and finite element methods [7, 8]. Several alternative but equivalent discrete mortar formulations exist [9]. Most implementations are based on the unconstrained saddle point approach since it allows for a local assembling. While mortar finite element formulations are quite often motivated by the flexibility of domain decomposition techniques or by the robustness with respect to non-matching meshes in dynamic applications, IGA leads in a natural way to a multi-patch situation in case of complex geometries, and mortar-type techniques are mandatory for the weak coupling see, e.g., [10, 11, 12]. A mathematical stability and a priori analysis enlightening the use of different dual spaces can be found in [13]. Higher-order couplings recently gained attention. We refer to [14, 15] for Kirchoff-Love shells. A discussion of strong C^1 couplings in multi-patch settings is given in [16], whereas weak continuity of the normal stress is realized in [17]. Alternative higher-order coupling methods based on least-squares techniques were proposed in [18].

Here, we investigate the influence of multi-patch coupling on the isogeometric eigenvalue approximation. As compared to IGA with maximal regularity, both weak and strong continuity couplings introduce outlier eigenvalues. This observation motivates us to propose a new hybrid mortar variant. In addition to the weak continuity satisfied in terms of a Lagrange multiplier, we apply a penalty approach for the jump terms in the higher derivatives. The weights in the penalization terms are selected such that both the condition number growth rate of the algebraic system and the optimal a priori convergence rate are preserved. The same approach is also successfully employed to cure the outliers produced when Neumann boundary conditions are imposed.

The paper is structured as follows: In Section 2, we briefly review the isogeometric mortar discretization, formulate the eigenvalue problem within the saddle point framework and introduce our hybrid mortar variant. Numerical results illustrate in Section 3 the influence of the penalization in the jump terms. In particular, the higher part of the spectrum can be significantly improved. Finally, in Section 4, conclusions are given.

2. Problem setting and hybrid mortar formulation

Let $\Omega \subset \mathbb{R}^d$, $d = 1, 2, 3$, be a bounded domain with $\bar{\Gamma}_D \cup \bar{\Gamma}_N = \partial\Omega$ and $\Gamma_D \cap \Gamma_N = \emptyset$. We consider the following Laplace eigenvalue problem with Dirichlet and

Neumann boundary conditions on Γ_D and Γ_N, respectively:

$$\begin{aligned} -\Delta u &= \lambda u, && \text{in } \Omega, \\ u &= 0, && \text{on } \Gamma_D, \\ \partial_n u &= 0, && \text{on } \Gamma_N. \end{aligned}$$

In the following, we briefly recapture isogeometric mortar methods, and for more details we refer to [13]. For the ease of presentation, we restrict ourselves to the two dimensional case. The generalization to one or three dimensions follows the same lines.

2.1. **Mortar saddle point formulation.** Let the domain Ω be decomposed into K non-overlapping subdomains Ω_k, i.e.,

$$\overline{\Omega} = \bigcup_{k=1}^{K} \overline{\Omega}_k, \text{ and } \Omega_i \cap \Omega_j = \emptyset, i \neq j.$$

Here, we limit our presentation to the basic isogeometric concepts and notations used throughout the paper and refer to the literature [5, 19, 20, 21] for more details. Each of the subdomains is a NURBS geometry, i.e., there exists a NURBS parametrization $\mathbf{F}_k$ based on an open knot vector $\boldsymbol{\Xi}_k$ and a degree p such that Ω_k is the image of the parametric space $\widehat{\Omega} = (0,1)^d$ by $\mathbf{F}_k$.

We set $N^p(\boldsymbol{\Xi}_k)$ as the multivariate NURBS space (corresponding to Ω_k) in the parametric domain, with the standard NURBS basis functions $\widehat{N}^p_{k,\mathbf{i}}$. For a set of control points $\mathbf{C}_{k,\mathbf{i}} \in \mathbb{R}^d$, $\mathbf{i} \in \mathbf{I}$, we define a parametrization of a NURBS surface as a linear combination of the basis functions and control points

$$\mathbf{F}_k(\boldsymbol{\zeta}) = \sum_{\mathbf{i} \in \mathbf{I}} \mathbf{C}_{k,\mathbf{i}}\, \widehat{N}^p_{k,\mathbf{i}}(\boldsymbol{\zeta}),$$

and assume the regularity stated in [22, Assumption 3.1].

For $1 \leq k_1 < k_2 \leq K$, we define the interface as the interior of the intersection of the boundaries, i.e., $\overline{\gamma}_{k_1 k_2} = \partial\Omega_{k_1} \cap \partial\Omega_{k_2}$, where $\gamma_{k_1 k_2}$ is open. Let the non-empty interfaces be enumerated by γ_l, $l = 1, \ldots, L$.

For each Ω_k, we introduce $H^1_*(\Omega_k) = \{v_k \in H^1(\Omega_k), v_{k|_{\partial\Omega \cap \partial\Omega_k}} = 0\}$, where we use standard Sobolev spaces, as defined in [23], endowed with their usual norms. In order to set a global functional framework on Ω, we consider the broken Sobolev space $V = \prod_{k=1}^K H^1_*(\Omega_k)$, endowed with the broken norm $\|v\|_V^2 = \sum_{k=1}^K \|v\|^2_{H^1(\Omega_k)}$. For any interface $\gamma_l \subset \partial\Omega_k$, we define by $H^{-1/2}(\gamma_l)$ the dual space of $H^{1/2}_{00}(\gamma_l)$, which is the space of all functions that can be trivially extended on $\partial\Omega_k \setminus \gamma_l$ by zero to an element of $H^{1/2}(\partial\Omega_k)$.

In the following, we set our non-conforming approximation framework. On each subdomain Ω_k, based on the NURBS parametrization, we introduce the approximation space $V_k = \{v_k = \widehat{v}_k \circ \mathbf{F}_k^{-1}, \widehat{v}_k \in N^p(\boldsymbol{\Xi}_k)\}$. On Ω, we define the discrete product space $V_h = \prod_{k=1}^K V_k \subset V$, which forms a $H^1(\Omega)$ non-conforming space discontinuous over the interfaces.

On the skeleton $\Gamma = \bigcup_{l=1}^L \gamma_l$, we define the discrete Lagrange multiplier product space M_h as $M_h = \prod_{l=1}^L M_l$. Based on the interface knot vector of one of the adjacent subdomains, M_l is a spline space of degree p defined on the interface γ_l. An appropriate local degree reduction performed at the crosspoints guarantees the inf-sup stability of the mortar coupling, see [13] for more details, while preserving optimal order error decay rates.

We define the bilinear forms $a\colon V \times V \to \mathbb{R}$ and $m\colon V \times V \to \mathbb{R}$, such that

$$a(u,v) = \sum_{k=1}^{K} \int_{\Omega_k} \nabla u \cdot \nabla v \, \mathrm{d}\mathbf{x}, \quad m(u,v) = \sum_{k=1}^{K} \int_{\Omega_k} u\, v \, \mathrm{d}\mathbf{x}$$

as well as

$$b(\tau, v) = \sum_{l=1}^{L} \int_{\gamma_l} \tau [v]_l \, \mathrm{d}\sigma,$$

where $[\cdot]_l$ denotes the jump over γ_l. The saddle point formulation of the isogeometric mortar eigenvalue problem reads as follows: Find $(u_h, \widehat{\tau}_h) \in V_h \times M_h$, $\lambda^h \in \mathbb{R}$, such that

$$\begin{aligned} a(u_h, v_h) + b(\widehat{\tau}_h, v_h) &= \lambda^h \, m(u_h, v_h), \quad v_h \in V_h, \\ b(\tau_h, u_h) &= 0, \quad \tau_h \in M_h, \end{aligned}$$

with the normalization $m(u_h, u_h) = 1$. The saddle point formulation introduces $2 \dim M_h$ spurious eigenvalues to the spectrum. We restrict ourselves to the physical relevant eigenpairs (λ^h, u_h). These are characterized by the fact that they are also eigenpairs of the constrained mortar formulation, i.e., they satisfy

$$a(u_h, v_h) = \lambda^h \, m(u_h, v_h), \quad v_h \in \{V_h : b(\tau_h, v_h) = 0, \tau_h \in M_h\}.$$

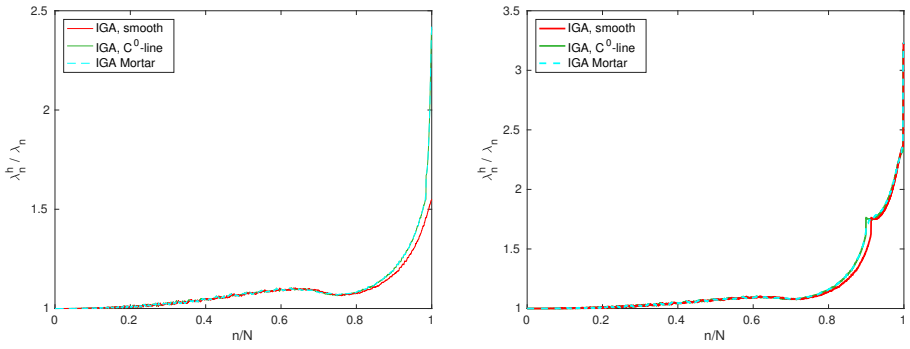

FIGURE 1. Normalized spectrum for $p = 2$. Left: Dirichlet BC. Right: Neumann BC.

To get a better feeling for the influence of the mortar coupling, we compare in Figure 1 three different IGA approaches for two different boundary conditions. As reference, we use the classical IGA approach with maximal regularity. Since we set $p = 2$, we have C^1-regularity. Additionally, we take into account the classical IGA approach with reduced regularity at the line $x = 1$, i.e., C^0-regularity (see [5, Chapter 3.5]), and the standard mortar IGA approach, i.e., continuity is only guaranteed in a weak sense, see Figure 5 for the used initial meshes. On the left, we show the normalized spectrum for Dirichlet boundary conditions on $\partial\Omega$. It can be seen that only the IGA approach with maximal regularity exhibits moderate outliers while both alternatives have more dominant outliers. The quality of the approximation is not significantly influenced by the choice of the continuity condition. Both options, strong or weak continuity, yield quantitatively the same results. However, the accuracy of the higher part in the spectrum is considerably improved if additionally strong continuity in the normal derivatives across the line $x = 1$ is imposed. On the right of Figure 1, we consider Neumann boundary conditions. Here all three approaches show severe outliers. We recall that in contrast to Dirichlet boundary

conditions, Neumann boundary conditions are typically not satisfied strongly but only weakly in a variationally consistent way.

These preliminary observations motivate us to impose higher regularity terms in the formulation. While on matching meshes strong C^1-continuity can be easily guaranteed, the situation is different for non-matching multi-patch meshes. Thus we impose higher regularity by additional penalty terms. As already mentioned weak C^1-continuity can be imposed in terms of an additional Lagrange multiplier approach. However this requires a careful selection of the space to guarantee uniform stability and involves a careful handling of the resulting algebraic system. Here we propose an alternative approach.

2.2. **Hybrid mortar formulation.** To improve the global continuity, we penalize the jump in the normal derivatives across the interfaces of a multi-patch geometry and the first normal derivative on a Neumann boundary part. To avoid locking, we take the local L^2-projection π_h^0 onto the piecewise constant functions on the (slave) boundary mesh.

The extra penalty term is given as

$$c_h(u_h, v_h) = C_{\mathrm{N}}\, c_{\mathrm{N}}(u_h, v_h) + \sum_{l=1}^{L} \sum_{m=1}^{p-1} C_l^m\, c_l^m(u_h, v_h) + C_{\mathrm{CP}}\, c_{\mathrm{CP}}(u_h, v_h)$$

with appropriate penalty constants $C_l^m, C_{\mathrm{N}}, C_{\mathrm{CP}} \geq 0$. The smooth interface coupling

$$c_l^m(u_h, v_h) = \int_{\gamma_l} h_s^{2m-1}\, \pi_h^0\left([\partial_n^m u_h]_l\right)\, \pi_h^0\left([\partial_n^m v_h]_l\right)\, \mathrm{d}\sigma,$$

as well as the Neumann penalty term

$$c_{\mathrm{N}}(u_h, v_h) = \int_{\Gamma_{\mathrm{N}}} h\, \pi_h^0\left(\partial_n u\right)\, \pi_h^0\left(\partial_n v\right)\, \mathrm{d}\sigma,$$

are properly weighted with the local mesh-size h_s on the slave side, respectively h on the boundary. The index CP in the bilinear form c_{CP} refers to contributions from the crosspoints. At the end points of each interface and each corner of the Neumann boundary, we introduce additional point evaluations. More precisely, for each interface γ_l, we add the term

$$\sum_{\bar{\mathbf{x}} \in \partial\gamma_l} \sum_{m=1}^{p-1} h_s^{2m} [\partial_n^m u_h]_l(\bar{\mathbf{x}}) [\partial_n^m v_h]_l(\bar{\mathbf{x}}).$$

On each corner $\bar{\mathbf{x}}$ of the Neumann boundary, the gradient is zero, so we add the term

$$h^2 \nabla u_h(\bar{\mathbf{x}}) \nabla v_h(\bar{\mathbf{x}}),$$

and for each point $\bar{\mathbf{x}}$, where an interface and the Neumann boundary intersect, we add the term

$$h^2 \partial_n u_h(\bar{\mathbf{x}}) \partial_n v_h(\bar{\mathbf{x}}),$$

where n indicates the outward normal.

We then consider the penalized eigenvalue problem

$$\begin{aligned} a_h(u_h, v_h) + b(\widehat{\tau}_h, v_h) &= \lambda^h\, m(u_h, v_h), \quad v_h \in V_h, \\ b(\tau_h, u_h) &= 0, \quad \tau_h \in M_h, \end{aligned}$$

with $a_h(u_h, v_h) = a(u_h, v_h) + c_h(u_h, v_h)$.

We now show broken H^1 continuity of the penalized bilinear form a_h and for $|\Gamma_D| > 0$ ellipticity on the kernel of the mortar coupling. The ellipticity trivially follows from the ellipticity of a, since

$$a_h(u_h, u_h) = a(u_h, u_h) + c_h(u_h, u_h) \geq a(u_h, u_h) \geq \alpha \|u_h\|_{V_h}^2.$$

To show continuity, it remains to prove $|c_h(u_h, v_h)| \leq C\|u_h\|_{V_h}\|v_h\|_{V_h}$. For the integral terms, using standard estimates and stability of the L^2-projection, this reduces to an inverse inequality $\|\partial_n^m v_h\|_{L^2(\gamma_l)} \leq Ch^{1/2-m}\|v_h\|_{H^1(\Omega_k)}$ for $m < p$.

For simplicity, we restrict ourselves to a single domain and one boundary part. Standard trace and inverse inequalities, see [19, Theorem 4.2], yield

$$\begin{aligned}\|\partial_n^m v_h\|^2_{L^2(\gamma_l)} &\leq C\|v_h\|_{H^m(\Omega_k)}\|v_h\|_{H^{m+1}(\Omega_k)} \\ &\leq Ch^{1-m}\|v_h\|_{H^1(\Omega_k)}h^{1-(m+1)}\|v_h\|_{H^1(\Omega_k)}.\end{aligned}$$

Noting that we have for polynomials an inverse inequality between L^∞- and L^2-norms, the point evaluations can be handled analogously.

Remark 1. *We note that the a priori analysis of the new hybrid mortar approach can be easily worked out within the abstract framework of non-conforming finite element techniques. The hybrid form allows us to use the Lemmata of Strang to show optimal order a priori bounds for right hand side problems and then further extend this to the eigenvalue theory analogously to* [24] *. We point out that the weights in the penalty term are selected such that the condition number of the algebraic system is still* $\mathcal{O}(h^{-2})$.

3. Numerical results

In this section, we present the eigenvalue approximation in different situations. In particular, after a systematical investigation in simple 1D and 2D settings, we study more complex 2D geometries composed of several patches, and we finally consider also a non-trivial multi-patch example in the framework of linear elasticity. The numerical simulations are based on the isogeometric Matlab toolbox GeoPDEs [25, 26]. We compare globally smooth spaces, C^0-couplings and the previously introduced higher-order penalty couplings. All results reported in the following are in terms of the normalized discrete eigenvalue λ^h/λ, which directly relates to the relative error in the eigenvalue since $(\lambda^h - \lambda)/\lambda = \lambda^h/\lambda - 1$. Note that in the case of pure Neumann boundary conditions, the first eigenvalue is zero, so we exclude it from the spectrum.

The numerically obtained eigenvalues can be grouped into physical relevant eigenvalues and spurious eigenvalues due to the coupling. We neglect these unphysical modes and only show the physical part of the resulting spectrum. The numerical criterion to distinguish between these parts is a relative criterion $\lambda^h_{n+1}/\lambda^h_n > 100$. We note that the spurious eigenvalues of the saddle point formulation are infinite.

For simple domains, analytical solutions are known for the eigenpairs, otherwise reference solutions need to be computed. On the unit line, the set of eigenvectors with pure Dirichlet conditions is given by $u_n(x) = \sqrt{2}\sin(n\pi x)$, with the corresponding eigenvalue $\lambda_n = n^2\pi^2$, $n = 1, 2, \ldots$, see [6]. In the Neumann setting we also have zero as eigenvalue. The two-dimensional eigenpairs on rectangles are obtained by a tensor product approach. We consider the two-dimensional domain $(0, 2) \times (0, 1)$, with eigenvalues

$$(n^2 + {n'}^2/4)\pi^2,$$

for $n, n' = 1, 2, \ldots$ in the pure Dirichlet case and $n, n' = 0, 1, \ldots$ in the pure Neumann case.

3.1. Single-patch 2D example with Neumann boundaries.

As we have seen, Neumann boundary conditions induce more significant outliers compared to the Dirichlet case. Thus, we first consider the discrete spectrum of a pure Neumann problem on a single-patch unit square with penalty. In Figure 2, the standard results for $p = 2$ are compared to those including a penalty for the Neumann

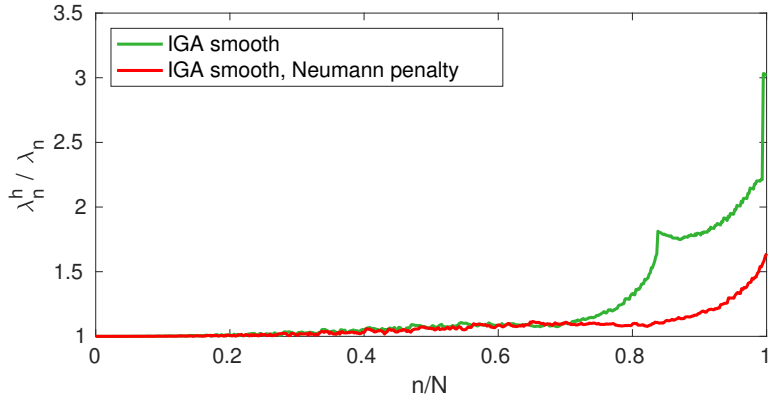

FIGURE 2. Single-patch 2D example with Neumann boundaries. Normalized discrete spectra for $p = 2$ with and without the Neumann boundary penalty.

conditions. We observe a considerable improvement, revealing the potential of the new hybrid variant.

By adding a penalty term measuring the violation of the Neumann boundary condition in a strong form, the complete spectrum can be approximated as good as in the Dirichlet case.

3.2. **One-dimensional results.** In this subsection, we report on one-dimensional results obtained with several higher-order penalty couplings.

	C^1	C^2	C^3	C^4
$\kappa^{\text{penalty}}/\kappa^{\text{kink}}, p = 2$	6.7e+02	-	-	-
$\kappa^{\text{penalty}}/\kappa^{\text{kink}}, p = 3$	1.1e+03	1.1e+03	-	-
$\kappa^{\text{penalty}}/\kappa^{\text{kink}}, p = 4$	1.6e+03	1.6e+03	2.6e+03	-
$\kappa^{\text{penalty}}/\kappa^{\text{kink}}, p = 5$	2.1e+03	2.8e+03	7.7e+03	7.7e+03

TABLE 1. Relative condition numbers for different ansatz and coupling degrees. Ratio of the condition number κ^{penalty} for the penalty coupling and the condition number κ^{kink} for the C^0-interface. Penalty constant chosen as $C_l^m = 10^{3-m}$.

In contrast to a pure penalty approach which typically leads to extremely poor condition numbers of the algebraic system, our hybrid variant is rather robust with respect to p. As already noted the condition number has the same growth rate as in the standard mortar setting. This results form the proper mesh dependent weighting. In Table 1, we consider the influence of p on the condition number. As reference we use an IGA approach with one C^0 point. The ratio depends sensitively on the choice of our penalty parameters but does not deteriorate as the mesh-size tends to zero. Furthermore it should be noted that by decreasing the penalty constant also the condition number decreases. However, also the magnitude of the spurious modes decreases and they get more close to the physical ones.

Figure 3 depicts the different discrete spectra of the pure Dirichlet problem using splines of degrees 2 and 3. A zoom into the higher frequency part of the spectra is also shown.

As it is well-known (see, e.g., [4]), finite elements fail to approximate the higher part of the spectrum while IGA with maximal regularity allows to obtain good

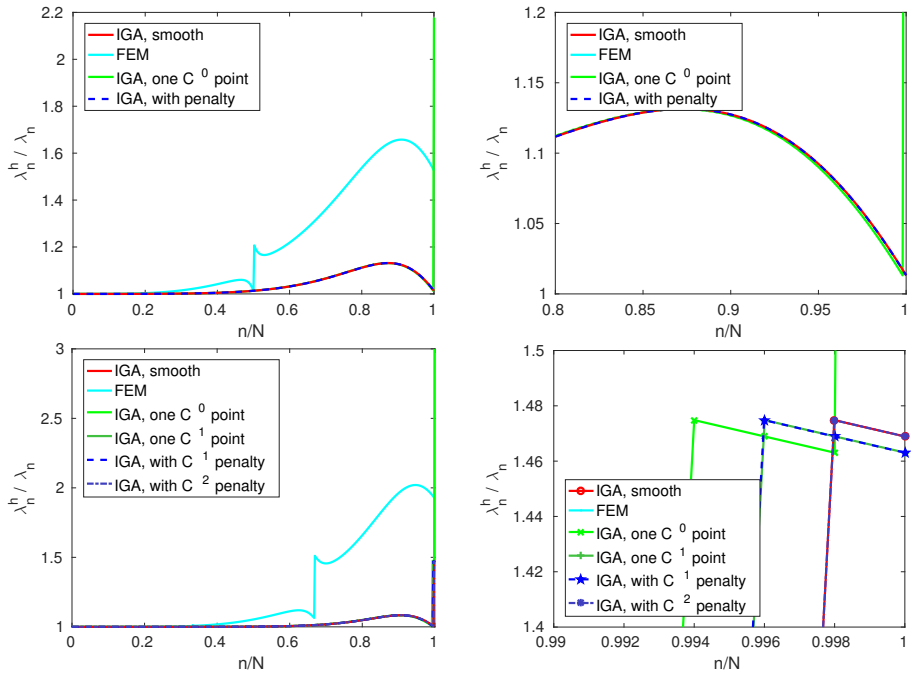

FIGURE 3. 1D Dirichlet problem: Top: $p = 2$, Bottom: $p = 3$. Left: Entire normalized discrete spectrum. Right: Zoom of the last part of the normalized discrete spectrum.

results. However IGA with reduced regularity, e.g., introduced by a C^0-line or by a weak mortar coupling across multiple-patches, also introduces outliers at the high frequency end of the spectrum. By our new hybrid variant which additionally penalizes jumps in the normal derivatives, the number of these outliers can be significantly reduced. We obtain quantitatively approximation quality as in the single-patch smooth case.

The results for the pure Neumann problem are shown in Figure 4, where we also see outliers for the smooth space. However, the penalty can reduce even these outliers and we end up with better results than with the original smooth spline space.

The results for degrees 4 and 5 are similar to those shown for degrees 2 and 3 and, therefore, are not reported here.

3.3. **Rectangular domain.** In this subsection, we show two-dimensional studies on two different mesh cases depicted in Figure 5, case (a), and Figure 6, case (b).

Figure 7 depicts the resulting normalized discrete spectra for the Dirichlet and the Neumann problems on the meshes of case (a). The IGA with maximal regularity and the IGA with a C^0-line are computed on the conforming mesh, whereas the weakly coupled mortar IGA approaches are computed on the nonconforming mesh. We test the cases $p = 2, 3, 4, 5$ and show only $p = 2, 5$.

In all cases, the lower frequency part of the spectrum is well approximated. In the higher frequency part of the spectrum (above 75%) we observe, as in the one dimensional case, a pollution of the approximation due to low-continuity couplings. In contrast to the one-dimensional case, these couplings do not just pollute a fixed number of modes, but a higher range of the spectrum due to the multivariate structure of the problem. Nevertheless it is observed that the outliers introduced by the weak or strong C^0-coupling can be avoided by including a penalization for

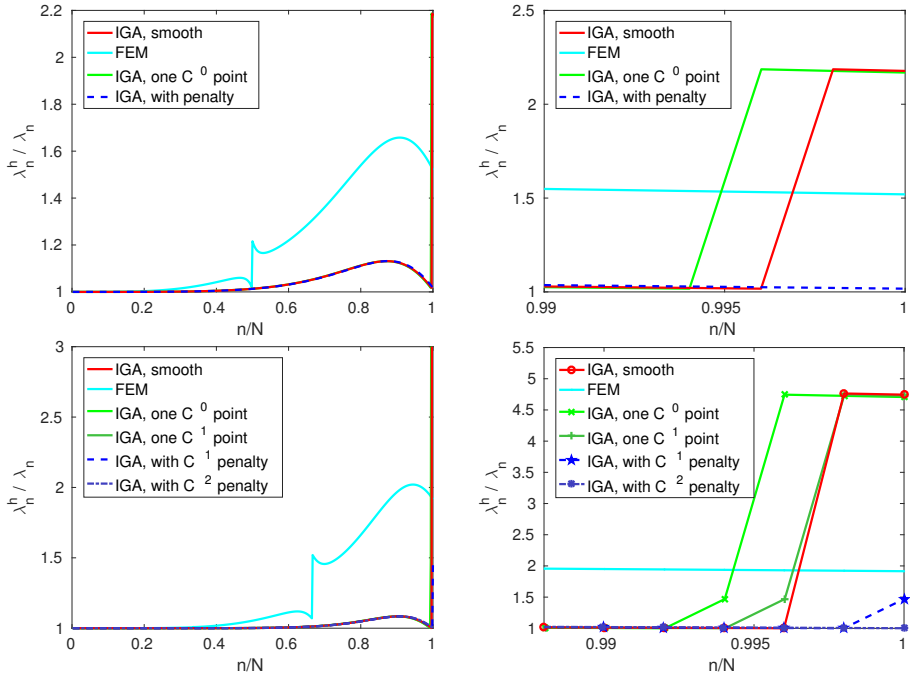

FIGURE 4. 1D Neumann problem: Top: $p = 2$, Bottom: $p = 3$. Left: Entire normalized discrete spectrum. Right: Zoom of the last part of the normalized discrete spectrum.

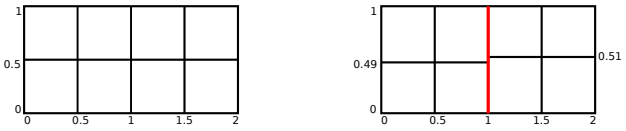

FIGURE 5. Mesh case (a). Conforming and nonconforming meshes.

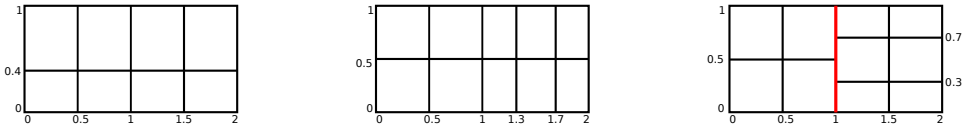

FIGURE 6. Mesh case (b). Left: First conforming mesh, Middle: Second conforming mesh, Right: Mortar mesh.

the jump terms in the normal derivatives. Only very few outliers which remain in some cases. For the Neumann problem, we observe the expected improvement of the outliers even in comparison to the IGA approach with maximal regularity, similar to the single-patch setting considered in Section 3.1.

For mesh case (b), the results depicted in Figure 8 are similar to mesh case (a). Furthermore, we observe an additional negative effect of mesh perturbation on the spectrum.

Remark 2. *The accurate evaluation of the mesh dependent bilinear form c_h requires, as the accurate evaluation of the mortar coupling bilinear form b, a suitable quadrature formula on a merged mesh. Here we use the same quadrature formula*

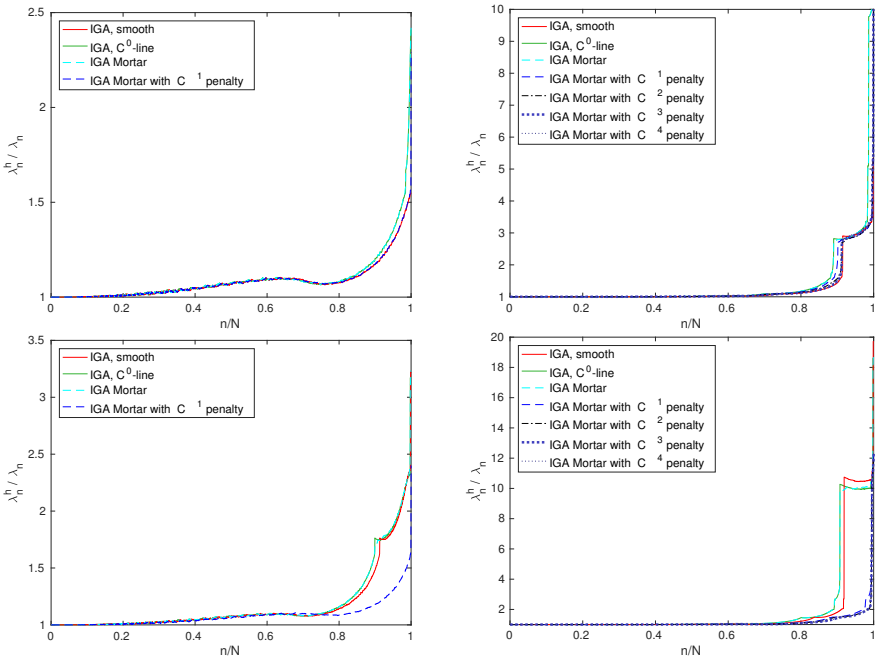

FIGURE 7. Normalized discrete spectrum for mesh case (a). Left: $p = 2$, Right: $p = 5$. Top: Dirichlet problem, Bottom: Neumann problem.

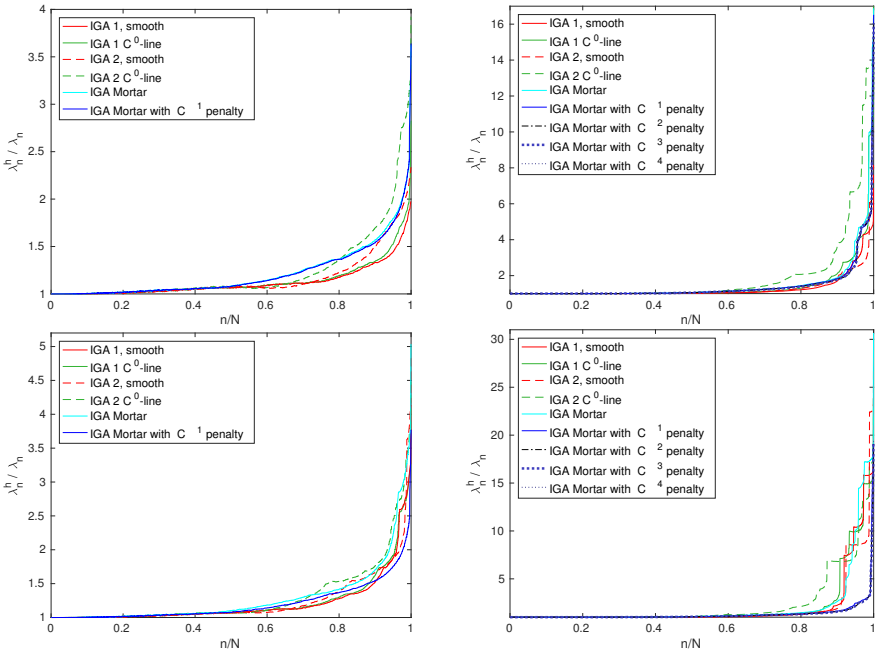

FIGURE 8. Normalized discrete spectrum for mesh case (b). Left: $p = 2$, Right: $p = 5$. Top: Dirichlet problem, Bottom: Neumann problem.

for both bilinear forms. More precisely a Gauss-quadrature with p+1 nodes per element is used on the merged mesh combining the boundary knots from the slave side

and the master side. This choice guarantees that the bilinear form b is evaluated exactly for B-splines on straight interfaces and order preserving in the more general case, see [13]*. We note that for the bilinear form c_h involving a L^2-projection onto constants a quadrature formula with less nodes for larger p is possible. While using a merged mesh for the evaluation of the bilinear form b is essential for the accuracy of the method, see* [27, 28, 29] *(which handle right-hand-side problems) the additional penalty terms are much less sensitive to variational crimes. Using for the evaluation of the bilinear form c_h a quadrature formula defined with respect to the slave mesh yields quantitatively the same good results while it reduces the extra computational cost. For $\mathbf{x} \in e_s$ a point on an element e_s of the slave-mesh, the projection $\pi_h^0(v_m)$ of a function v_m on the master side, is evaluated as follows. Let $\mathbf{x}_q^{e_s}, q = 1, \dots, \lceil (p+1)/2 \rceil$, be the Gauss-points on e_s with weights ω_q, then we approximate*

$$\pi_h^0(v_m)(\mathbf{x}_s) \approx \sum_{q=1}^{\lceil (p+1)/2 \rceil} \omega_q v_m(\mathbf{x}_q^{e_s}).$$

The remaining integral of piecewise constants on the slave mesh can trivially be computed exactly.

3.4. **Multi-patch examples with crosspoints.** Let us now consider a non-affine geometry mapping and a non-convex domain. We consider an annulus defined by: $\{\mathbf{x} \in \mathbb{R}^2 : 1/2 < |\mathbf{x}| < 1\}$. Homogeneous Dirichlet boundary conditions are applied to the inner boundary part, i.e., $|\mathbf{x}| = 1/2$, Neumann boundaries on the remaining parts.

The geometry no longer allows for a smooth coupling-free discretization. We therefore consider the four smooth patches shown in Figure 9 (left), where non-matching meshes were constructed by knot insertion. We consider quadratic splines

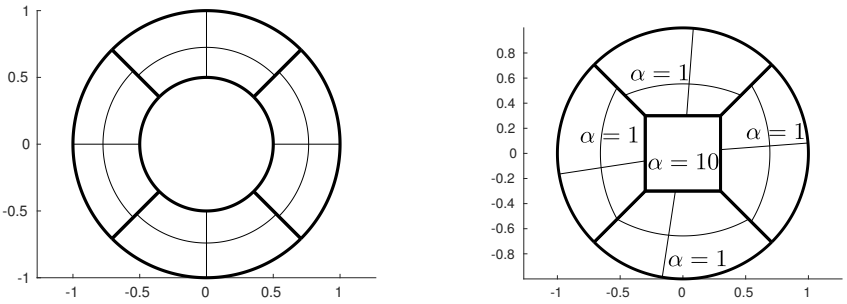

FIGURE 9. Initial mesh and geometry decomposition of the considered non-trivial multi-patch examples. Left: Annulus. Right: Bimaterial disk.

after four uniform mesh refinements. The resulting eigenvalue approximation is shown in Figure 10 (left), where we can see a better approximation of the spectrum obtained with the C^1 penalty coupling in comparison to the original mortar coupling. Only very few outliers remain with a comparably smaller magnitude.

The second example introduced in Figure 9 (right) is a bimaterial unit disk constituted by five patches with pure Neumann boundary conditions. Here we alter the Laplace equation and solve $-\operatorname{div} \alpha \nabla u = \lambda u$, where $\alpha = 1$ in the four outer patches and $\alpha = 10$ in the inner one. We note that the normal derivative must be replaced by $\alpha \partial_n u$ since the material jump induces a kink in the exact solution. Quadratic splines are considered after three uniform mesh refinements. The results reported in Figure 10 (right) show that the maximal outlier is reduced to almost half of its value.

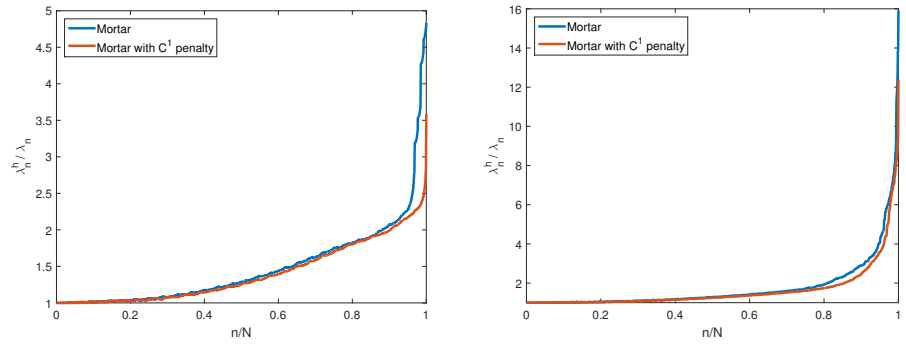

FIGURE 10. Normalized discrete spectra for the considered non-trivial multi-patch examples. Left: Annulus. Right: Bimaterial disk.

3.5. **Application to linear elasticity.** Finally, we apply the penalty method to a non-trivial example of elasticity. We consider a beam, with three circular cut-outs, as depicted in Figure 11, clamped on the left side, with Neumann boundaries on the remaining edges including the circular holes.

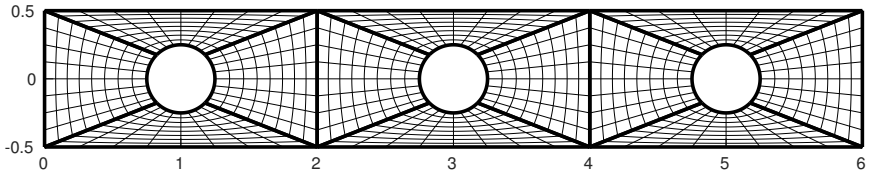

FIGURE 11. Linear elastic beam with circular cut-outs and its decomposition into patches.

We solve the eigenvalue problem of linear elasticity:

$$\begin{aligned} -\operatorname{div}\sigma(u) &= \lambda u, \quad && \text{in } \Omega, \\ u &= 0, && \text{on } \Gamma_D, \\ \sigma(u)\cdot n &= 0, && \text{on } \Gamma_N, \end{aligned}$$

where the linearized stress and strain is given by $\sigma(u) = 2\bar{\mu}\varepsilon(u) + \bar{\lambda}\operatorname{tr}\varepsilon(u)I$ and $\varepsilon(u) = 1/2(\nabla u + \nabla u^\top)$, respectively. The Lamé parameters depend on the elastic modulus $E = 1$ and Poisson's ratio $\nu = 0.3$ by

$$\bar{\mu} = \frac{E}{2(1+\nu)}, \quad \bar{\lambda} = \frac{\nu E}{(1+\nu)(1-2\nu)}.$$

For the equations of elasticity, the surface traction $\sigma(u)\cdot n$ plays the role of the normal derivative in the Laplace setting. Hence, the normal derivative in the penalty terms is replaced by $\sigma(u)\cdot n$ on the Neumann boundary as well as on the interfaces.

The results for a quadratic discretization are shown in Figure 12. We see that the proposed method provides a significant overall improvement of the discrete spectrum also in the framework of elasticity. In particular, the maximal outlier is reduced to approximately half of its value.

4. CONCLUSIONS

In this paper, we have studied, in the framework of isogeometric analysis, the effects of multi-patch geometries and Neumann boundaries on the approximation

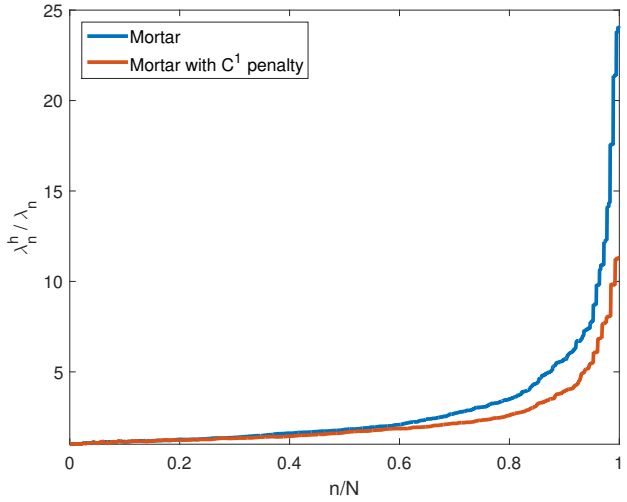

FIGURE 12. Normalized discrete spectra for the linear elastic beam with circular cut-outs.

of eigenvalue problems. The so-called outlier eigenvalues produced in these cases negatively affect the approximation of the high frequency part of the spectrum. This part of the spectrum is relevant in several applications such as, e.g., explicit dynamics. We herein present a simple and effective hybrid approach as remedy. Adding penalty terms for the jumps in the normal derivatives at the Neumann boundary and the multi-patch interfaces yields significantly better results. The mesh-dependent weights in the penalty terms are selected such that uniform stability and optimal order a priori bounds hold. Numerically it is observed that these penalty terms are much less sensitive to the choice of the quadrature formulas. In contrast to the weak variational consistent Lagrange multiplier continuity coupling, it is sufficient to define the applied quadrature formula on the mesh of the slave side. A systematical study of the good behavior of the proposed method has been carried out in the framework of Laplace problems in the case of simple 1D and 2D geometries. In addition, a number of more complex mapped multi-patch examples have been successfully tackled, also in the context of linear elasticity.

REFERENCES

[1] T. J. R. Hughes, J. A. Cottrell, Y. Bazilevs, Isogeometric analysis: CAD, finite elements, NURBS, exact geometry and mesh refinement, Comput. Methods. Appl. Mech. Eng. 194 (2005) 4135–4195.

[2] K. Höllig, Finite Element Methods with B-Splines, Frontiers in Applied Mathematics, SIAM, 2003.

[3] J. Cottrell, A. Reali, Y. Bazilevs, T. Hughes, Isogeometric analysis of structural vibrations, Comput. Methods Appl. Mech. Eng. 195 (4143) (2006) 5257 – 5296.

[4] T. Hughes, A. Reali, G. Sangalli, Duality and unified analysis of discrete approximations in structural dynamics and wave propagation: Comparison of p-method finite elements with k-method NURBS, Comput. Methods Appl. Mech. Eng. 197 (4950) (2008) 4104 – 4124.

[5] J. A. Cottrell, T. J. R. Hughes, Y. Bazilevs, Isogeometric Analysis. Towards Integration of CAD and FEA, Wiley, Chichester, 2009.

[6] T. J. Hughes, J. A. Evans, A. Reali, Finite element and NURBS approximations of eigenvalue, boundary-value, and initial-value problems, Comput. Methods Appl. Mech. Eng. 272 (2014) 290 – 320.

[7] F. Ben Belgacem, The mortar finite element method with Lagrange multipliers, Numer. Math. 84 (1999) 173–197.

[8] C. Bernardi, Y. Maday, A. T. Patera, A new nonconforming approach to domain decomposition: the mortar element method, in: H. B. et.al. (Ed.), Nonlinear partial differrential equations and their applications., Vol. XI, Collège de France, 1994, pp. 13–51.
[9] B. Wohlmuth, Discretization Techniques and Iterative Solvers Based on Domain Decomposition, Vol. 17, Springer, Heidelberg, 2001.
[10] A. Apostolatos, R. Schmidt, R. Wüchner, K.-U. Bletzinger, A Nitsche-type formulation and comparison of the most common domain decomposition methods in isogeometric analysis, Int. J. Numer. Methods Eng. 97 (2014) 473–504.
[11] W. Dornisch, G. Vitucci, S. Klinkel, The weak substitution method an application of the mortar method for patch coupling in NURBS-based isogeometric analysis, International Journal for Numerical Methods in Engineering 103 (3) (2015) 205–234.
[12] C. Hesch, P. Betsch, Isogeometric analysis and domain decomposition methods, Comput. Methods Appl. Mech. Eng. 213–216 (2012) 104–112.
[13] E. Brivadis, A. Buffa, B. Wohlmuth, L. Wunderlich, Isogeometric mortar methods, Comput. Methods Appl. Mech. Eng. 284 (2015) 292–319.
[14] J. Kiendl, K.-U. Bletzinger, J. Linhard, R. Wüchner, Isogeometric shell analysis with Kirchhoff-Love elements, Comput. Methods Appl. Mech. Eng. 198 (4952) (2009) 3902 – 3914.
[15] J. Kiendl, Y. Bazilevs, M.-C. Hsu, R. Wüchner, K.-U. Bletzinger, The bending strip method for isogeometric analysis of Kirchhoff-Love shell structures comprised of multiple patches, Comput. Methods Appl. Mech. Eng. 199 (3740) (2010) 2403 – 2416.
[16] R. Bouclier, J.-C. Passieux, M. Salaün, Development of a new, more regular, mortar method for the coupling of NURBS subdomains within a NURBS patch: Application to a non-intrusive local enrichment of NURBS patches, Comput. Methods Appl. Mech. Eng., published online.
[17] A. Collin, G. Sangalli, T. Takacs, Analysis-suitable G^1 multi-patch parametrizations for C^1 isogeometric spaces, Computer Aided Geometric Design 47 (2016) 93 – 113.
[18] L. Coox, F. Greco, O. Atak, D. Vandepitte, W. Desmet, A robust patch coupling method for NURBS-based isogeometric analysis of non-conforming multipatch surfaces, Comput. Methods Appl. Mech. Eng., published online.
[19] Y. Bazilevs, L. Beirão da Veiga, J. A. Cottrell, T. J. R. Hughes, G. Sangalli, Isogeometric analysis: Approximation, stability and error estimates for h-refined meshes, Math. Models Methods Appl. Sci. 16 (7) (2006) 1031–1090.
[20] L. Piegl, W. Tiller, The NURBS Book, Springer, 1997.
[21] L. Schumaker, Spline Functions: Basic Theory, 3rd Edition, Cambridge University Press, Cambridge, 2007.
[22] L. Beirão Da Veiga, A. Buffa, G. Sangalli, R. Vásquez, Mathematical analysis of variational isogeometric methods, Acta Numerica 23 (2014) 157–287.
[23] P. Grisvard, Elliptic Problems in Nonsmooth Domains, SIAM, Philadelphia, 2011.
[24] I. Babuška, J. Osborn, Eigenvalue problems, in: P. Ciarlet, J. Lions (Eds.), Handbook of Numerical Analysis, Vol. 2, Elsevier, 1991, pp. 641–787.
[25] C. de Falco, A. Reali, R. Vásquez, GeoPDEs: A research tool for isogeometric analysis of PDEs, Adv. Eng. Softw. 42(12) (2011) 1020–1034.
[26] R. Vázquez, A new design for the implementation of isogeometric analysis in Octave and Matlab: GeoPDEs 3.0, Tech. Rep. 16-02, IMATI-CNR, Pavia (April 2016).
[27] L. Cazabeau, C. Lacour, Y. Maday, Numerical quadrature and mortar methods, in: Computational Science for the 21st Century, John Wiley and Sons, 1997, pp. 119–128.
[28] Y. Maday, F. Rapetti, B. I. Wohlmuth, The influence of quadrature formulas in 2D and 3D mortar element methods., in: Recent developments in domain decomposition methods. Some papers of the workshop on domain decomposition, ETH Zürich, Switzerland, June 7–8. 2001, Springer, 2002, pp. 203–221.
[29] E. Brivadis, A. Buffa, B. Wohlmuth, L. Wunderlich, The influence of quadrature errors on isogeometric mortar methods, in: B. Jüttler, B. Simeon (Eds.), Isogeometric Analysis and Applications 2014, Springer International Publishing, Cham, 2015, pp. 33–50.